# Tailored Control Strategy for Ejector-equipped Transcritical R744 Heat Pumps for Milk Processing

*Victor M. Fontalvo[a,b], Danial Sattari[a], Rakesh T. Ganesh[a], Krester Kjær Sørensen[c] and Paride Gullo[a]*

[a] *University of Southern Denmark (SDU), Sønderborg, Denmark, parigul@sdu.dk*
[b] *Universidad de Magallanes, Punta Arenas, Chile, vfmorales@sdu.dk, CA*
[c] *Bitzer Electronics A/S, Sønderborg, Denmark, kresten.soerensen@bitzerdk.com*

**Abstract:**
Milk processing is an essential step in the dairy chain, as it ensures safety, quality and longer shelf life of products. Yet this process is also energy intensive, requiring significant heating (still widely provided via fossil fuel-based boilers), cooling and cleaning operations.
Ejector-equipped transcritical $CO_2$ (R744) heat pumps are an environmentally friendly and efficient alternative to fossil fuel-based boilers in the dairy sector, while simultaneously meeting their cooling needs. However, they require a specific control strategy to precisely manage their high pressure and maximise the coefficient of performance (COP) across all operating conditions. Therefore, in this work a real-time control algorithm was developed and tested in a simulation environment of a realistic ejector-equipped transcritical R744 heat pump operating in a milk processing plant under dynamic loads and disturbances. The selected case study involved a cooling demand at 4 °C for milk chilling and a heating demand at 72 °C for milk pasteurisation. The results showed that the developed correlation for the optimal high pressure can maximize the heat pump energy efficiency in real time as a function of the evaporator pressure and the gas cooler/condenser R744 outlet temperature. Also, it was found that the correlation increases the daily averaged COP by about 2.3 % on both considered days (8 February and 4 August) compared to the non-optimal conditions in Hobro (Denmark). Finally, the use of the optimal correlation for the high pressure decreased the useful energy cost by about at least 3 % on the selected days, while increasing the cooling load by 28 % compared to the scenario featuring the same heating load.

**Keywords:**
Carbon Dioxide, Control Logic, Dynamic Modelling, Ejector, Energy Efficiency, Performance Optimisation.

# 1. Introduction

The cold chain is estimated to account for about 4 % of global greenhouse gas (GHG) emissions, underscoring the urgent need for more environmentally friendly solutions for processing, preserving and transporting products. Therefore, the first step towards decarbonising this sector is to minimise the use of fossil fuel-based boilers and increase the adoption of ultra-low global warming potential (GWP) refrigerants.

The dairy industry is one of the most crucial sectors of the cold chain, requiring both cooling and heating for milk storage, cleaning-in-place (CIP) and milk processing. On the one hand, heating demand is currently mostly met by fossil fuel-based boilers. On the other hand, vapour-compression systems can simultaneously and sustainably satisfy heating and cooling demands, thereby reducing boiler use. The simultaneous adoption of a two-phase ejector for expansion work recovery and carbon dioxide (R744) as the sole refrigerant in heat pumps for simultaneous cooling and heating can yield enormous energy and environmental advantages over boilers, while also meeting cooling demand. The study by Singh and Dasgupta [1] revealed that a transcritical R744 heat pump employed in a milk processing facility and using the waste heat from a R747 refrigeration unit can reduce the fuel consumption and the GHG emissions by up to 45.7 % and 33.8 % and offer a payback time of 40 months. However, precise control of the high pressure of ejector-equipped R744 heat pumps and thus a dedicated control algorithm is required [2]. To the best of the authors' knowledge, the only work on the optimal control of ejector-equipped R744 heat pumps is that of Liu et al. [3]. The results obtained showed that the proposed multi-objective dynamic optimal control strategy can substantially improve the system COP.

Therefore, this study aims to develop a preliminary dedicated control algorithm for ejector-equipped R744 heat pumps. A milk processing factory requiring cooling at 4 °C for milk chilling and heating from 60 °C to 72 °C for milk pasteurisation [4] was used as the case study. Firstly, the operating parameters that most strongly influence the optimal high pressure were identified. Then, a dedicated correlation for the optimal high pressure was developed and implemented in the heat pump control system. Thus, the control system performance was assessed over 24 hours in 2 different days (8 February and 4 August) in Hobro (Denmark). Finally, the energy and economic benefits were quantified on the two aforementioned days based on the actual electricity price.

The work is organized as follows: the investigated system, the mathematical model, the assumptions made and the control logic are described in Section 2, while the results are presented in Section 3. Finally, the conclusions are summarized in Section 4.

# 2. Materials and Methods

## 2.1. System Description

The investigated heat pump for simultaneous cooling and heating is schematized in Figure 1. The ejector is employed to pre-compress R744 from the evaporator pressure to the receiver pressure, thereby increasing the compressor suction pressure and consequently enhancing the heat pump energy efficiency. The refrigerant leaving the ejector enters the receiver where vapour phase and liquid one are separated. The saturated liquid at the bottom of the receiver is then isenthalpically expanded in the expansion valve, before it vaporizes at 0 °C (for milk chilling) in the evaporator and the superheated vapour is drawn by the ejector suction nozzle. The saturated vapour at the top of the receiver is drawn by the compressor and enters the de-superheater to heat the cooling medium from 60 °C up to 72 °C (for milk pasteurisation). Finally, the refrigerant exiting the de-superheater is further cooled down in the air-cooled gas cooler/condenser before it goes into the ejector motive nozzle.

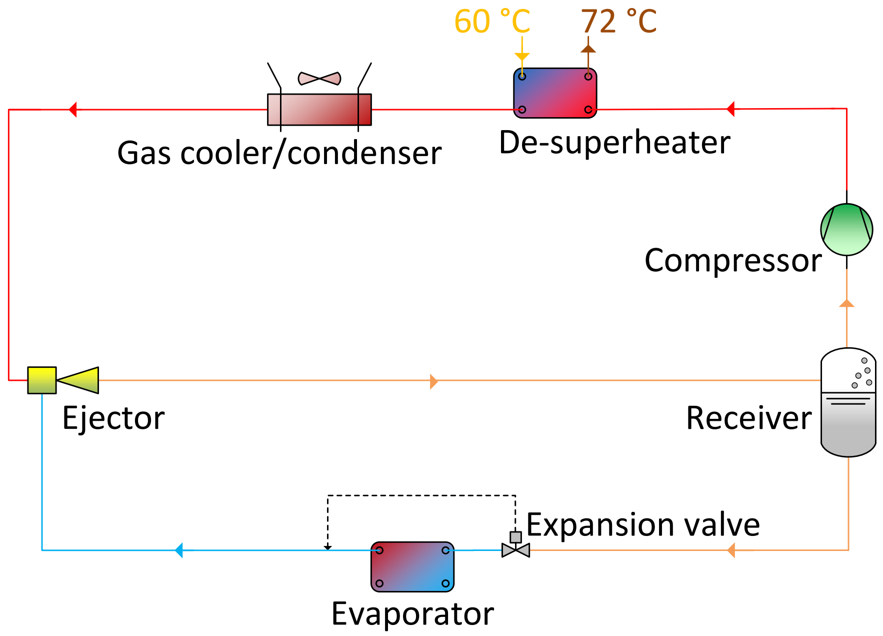


***Figure 1.*** *Schematic of the investigated heat pump.*

## 2.2. Mathematical Model and Assumptions

A regression analysis was developed using Engineering Equation Solver (EES) [5] to evaluate the optimal high pressure  that maximises the COP as a function of various operational parameters across all operating conditions. The analysis was carried out by assuming the heat pump was operating under steady-state conditions and applying energy and mass balances to each component.

As for the dynamic simulations, the components were modelled using the manufacturers' datasheets. The dynamic simulation model was implemented in the MATLAB/Simulink platform [6] and all thermo-physical properties were evaluated using CoolProp [7].

In all cases, the ejector was modelled according to [8] imposing a pressure lift between 2 bar and 10 bar and the developed simulation models were based on the following assumptions:

- negligible heat gains/losses related to the components;
- negligible pressure drops in the heat exchangers and pipes;
- negligible kinetic (except for the ejector) and potential energy variations in the components;
- expansion process within all the expansion valve was assumed to be isenthalpic.

For the analysed heat pump, the COP was defined as:

$$COP = \frac{\dot{Q}_{evap}+\dot{Q}_{des}}{\dot{W}_{comp}}, \quad (1)$$

in which $\dot{Q}_{evap}$ is the cooling load in the evaporator, $\dot{Q}_{des}$ is the heating load provided to the milk pasteurisation through the de-superheater and $\dot{W}_{comp}$ is the compressor power input; all in kW.

## 2.3 Setpoints and Control Strategy Development

The control strategy of the heat pump was based on:

- the evaporator expansion valve controlling the superheating degree;
- the ejector setting the high pressure to the value maximizing the COP at any operating condition;
- a pump on the cooling medium side controlling the de-superheater outlet temperature at 72 °C;
- a pump on the secondary fluid side setting the evaporator temperature to 0 °C;
- the compressor controlling the heating load.

Due to strong interactions among the loops, careful tuning was needed to avoid overly oscillatory responses.

## 2.4 Optimal High pressure

Several operating conditions were analysed to develop a correlation for the optimal high pressure maximizing the COP. For each condition, the optimal high pressure was varied between 75 bar and 110 bar and determined using the Genetic Method in EES based on the open-access Pikaia optimisation program. This method was used to ensure that the global optimum was found even when a local optimum exists. A $2^k$ design of experiment (DOE) was employed with the factors and the limits presented in Table 1.

***Table 1.*** *Factors and levels for the $2^k$ DOE.*

| Factor | Lower limit | Upper limit |
|---|---|---|
| A - Evaporator superheating degree (K) | 8 | 15 |
| B - Compressor efficiency (%) | 50 | 70 |
| C - De-superheater R744 outlet temperature (°C) | 62 | 72 |
| D - Gas cooler/condenser R744 outlet temperature (°C) | 22 | 30 |
| E - Evaporator pressure (bar) | 34 | 40 |

# 3. Results and Discussion

Firstly, the key results for each model of each component were compared with those in the manufacturer data sheets. It was found that the compressor discharge temperatures and power inputs can be estimated with a maximum and mean absolute error of 1.4 % and 0.7 %, and 3.1 % and 1.9 %, respectively. Also, the maximum error in calculating the R744 temperature at the outlet of the gas cooler/condenser was 0.8 %, resulting in a mean absolute error of 0.4 %. The mean absolute error for the corresponding heating load and the outlet cooling medium temperature was 0.2 % and 0.1 %, respectively. Finally, the mass flow rate through the expansion valve was computed with a mean absolute error of 0.2 %.

## 3.1 Development of the Optimal High pressure

According to the DOE, 32 operational points were considered, and each factor and its interactions were evaluated for significance using an analysis of variance (ANOVA). The results summarised in Table 2 suggested that only the gas cooler/condenser R744 outlet temperature, the evaporator pressure and their interaction (indicated as DE in Table 2) significantly affect the optimal high pressure value.

***Table 2.*** *ANOVA for the $2^k$ DOE.*

| Source | Sum of Squares | df | Mean Square | F-Value | p-value Prob > F |
|---|---|---|---|---|---|
| Model | 6440,815 | 3 | 2146,938 | 40076,182 | < 0.0001 |
| D - Gas cooler/condenser R744 outlet temperature (°C) | 6171,605 | 1 | 6171,605 | 115203,293 | < 0.0001 |
| E - Evaporator pressure (bar) | 142,805 | 1 | 142,805 | 2665,693 | < 0.0001 |
| DE | 126,405 | 1 | 126,405 | 2359,560 | < 0.0001 |
| Residual | 1,5 | 28 | 0,05357143 | | |
| Cor Total | 6442,315 | 31 | | | |

The outcomes presented in Figure 2 indicate that low gas cooler/condenser R744 outlet temperatures and high evaporator pressure s were preferred to maximise the COP, resulting in the additional benefit of reducing the optimal high pressure . Also, it was observed that at higher gas cooler/condenser R744 outlet temperatures, the optimal high pressure was less sensitive to changes in evaporator pressure. Still, it also yielded higher optimal high pressure values and, therefore, more thermally and mechanically stressful operational conditions for the heat pump. Finally, at lower gas cooler/condenser R744 outlet temperatures, a higher evaporator pressure could slightly improve the COP.

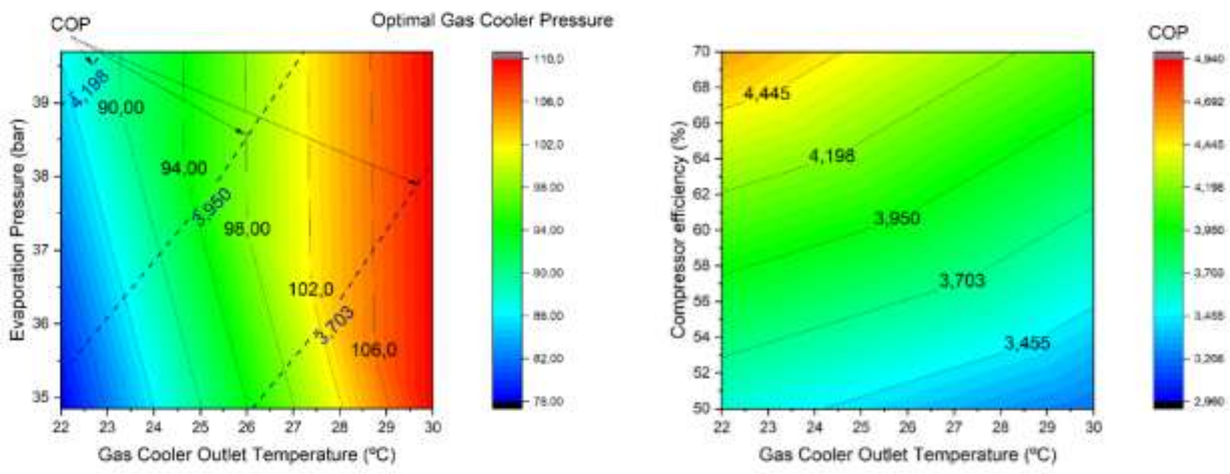


***Figure 2. Influence of the gas cooler/condenser R744 outlet temperature and evaporator pressure on the optimal high pressure (left), influence of the gas cooler/condenser R744 outlet temperature and compressor efficiency on the COP (right).***

After this initial screening, recalling that the gas cooler/condenser R744 outlet temperature ($T_{GC\ out}$) and the evaporator pressure ($P_{evap}$) are the variables that influence the optimal high pressure ($P_{high}^{optimal}$) the most, a new optimisation was carried out and extended to the dynamic model developed in Simscape/MATLAB. A central composite design was used for these variables, resulting in 9 operational scenarios.

***Table 3.*** *ANOVA for the proposed regression.*

| | df | Sum of Squares | Mean Square | F Value | p-value Prob > F |
|---|---|---|---|---|---|
| Regression | 6 | 61102.94 | 10183.82 | 1034.16 | 4.74E-05 |
| Residual | 3 | 29.54 | 9.85 | | |
| Uncorrected Total | 9 | 61132.48 | | | |
| Corrected Total | 8 | 222.24 | | | |
| | | | | | |
| $R^2$ | 0.8671 | | | | |

From Table 3, it can be concluded that the regression performed significantly better at describing the optimal pressure of the gas cooler than a fixed value. The obtained correlation for the optimal high pressure is represented by the full quadratic model in Equation (2):

$$P_{high}^{optimal}\,(bar) = 68.297 - 1.055T_{GC\ out} + 1.848P_{evap} + 0.07489T_{GC\ out}^2 + 0.04217P_{evap}^2 - 0.12558T_{GC\ out}P_{evap} \qquad (2)$$

in which $T_{GC}$ is the gas cooler/condenser R744 outlet temperature in °C, $P_{evap}$ is the evaporator pressure , and $P_{high}^{optimal}$ is the optimal high pressure, both in bar.

Figure 3 shows the predicted optimal high pressure based on correlation compared with data points from the nine scenarios considered in the dynamic simulation. This response surface indicated that the gas cooler/condenser R744 outlet temperature and evaporator pressure have a directly proportional effect on the optimal high pressure. Additionally, from Eq. (2) and Figure 3, it can be concluded that the interaction between these variables was significant, as evidenced by the curvature of the response surface.

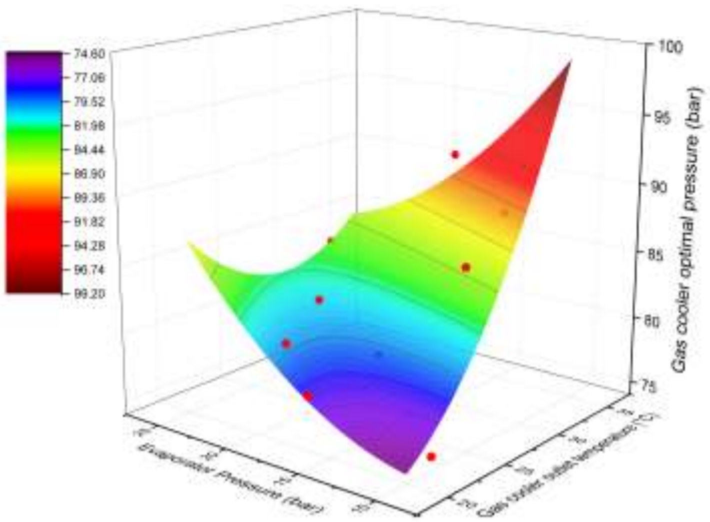


***Figure 3. Influence of the gas cooler/condenser R744 outlet temperature and evaporator pressure on the optimal high pressure (red dots) and predicted optimal high pressure (RSM).***

## 3.2 Control System Performance Evaluation

For the control system performance test, two representative daily temperature profiles in Hobro (Denmark), i.e., 8 February and 4 August, were selected (see Figure 3, left). The gas cooler/condenser R744 outlet temperature setpoint was set to 25°C, while the high pressure for the not optimized scenario was taken as 83 bar. On both days the gas cooler/condenser temperature setpoint could be achieved, except during heat load setpoint changes; however, the deviation from the setpoint during operation was greater in August, averaging 4.3 K, compared with 3.4 K in February. This could be attributed to the lower air temperature, which enhanced the heat transfer in the gas cooler/condenser.

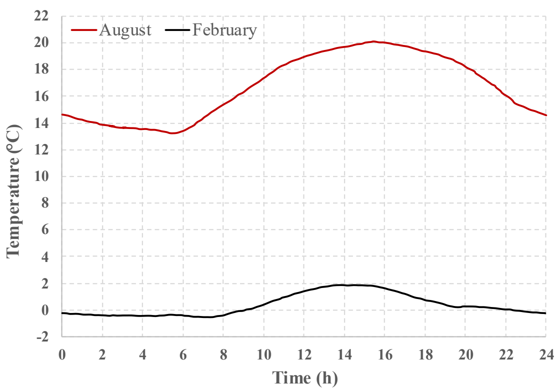


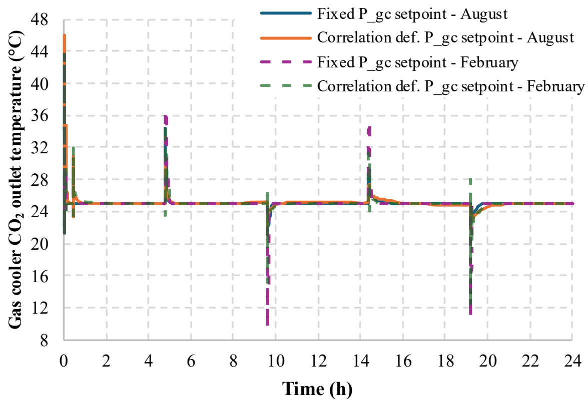


***Figure 4.  Air temperature (left) and gas cooler/condenser R744 outlet temperature (superheating degree = 10 K).***

In Figure 5, the results indicated that the system can adjust its high pressure in real time contingent upon the instantaneous evaporator pressure  and the gas cooler outlet temperature. As expected, fluctuations in this pressure were most pronounced during variations in heating load coinciding with periods when the gas cooler/condenser R744 outlet temperature exhibited the greatest deviations. Figure 6 shows that during the daytime the system could seamlessly follow the changes in the heating load. However, a noticeably greater overshoot occurred when a heat load change happened during system operation with a variable high pressure, in both August and February. This phenomenon could be attributed to the strong interaction between the high pressure and the ejector opening degree, being the expansion work recovery device responsible for controlling the high pressure. Also, this effect was more pronounced when implementing the optimal high pressure approach due to the influence of the evaporator pressure, which was also affected by the compressor dynamic response on the optimal high pressure setpoint. As heat loads and RPM increased, the evaporator pressure tended to decrease and consequently their control loops required further analysis and tuning to minimise their interactions.

Remembering that the proposed system was intended for both heating and cooling processes, the cooling load dynamic response is presented in Figure 7. Both thermal loads were strongly related, so changing one was found to affect the other. It was observed that for the same heating load a greater cooling load can be achieved when the high pressure is optimised and the COP is greater than that of the baseline, i.e., fixed high pressure scenario.

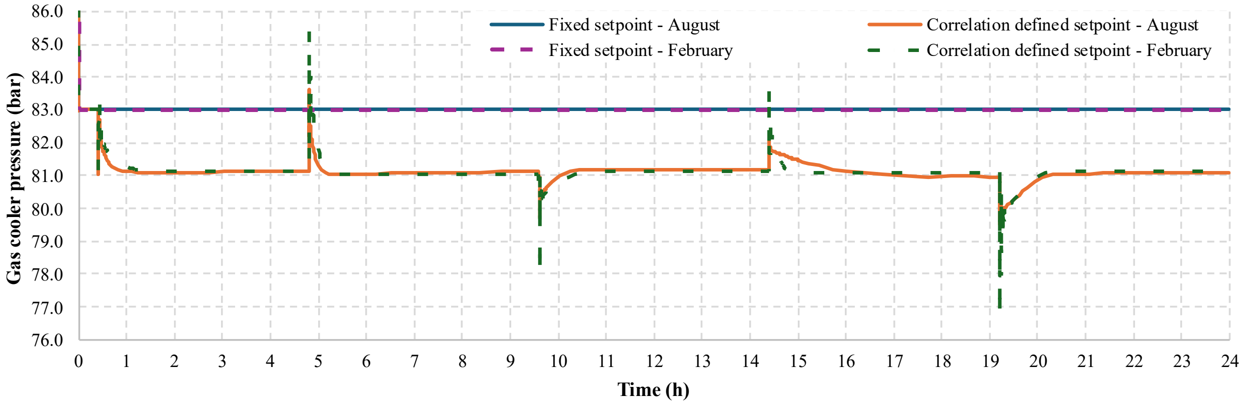


***Figure 5.*** *High pressure dynamic response (superheating degree = 10 K).*

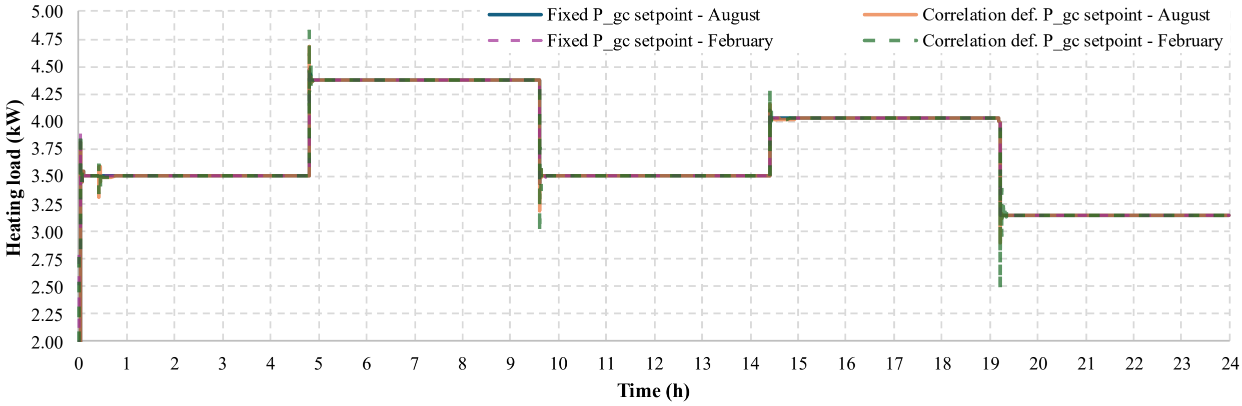


***Figure 6.*** *Heating load dynamic response (superheating degree = 10 K).*

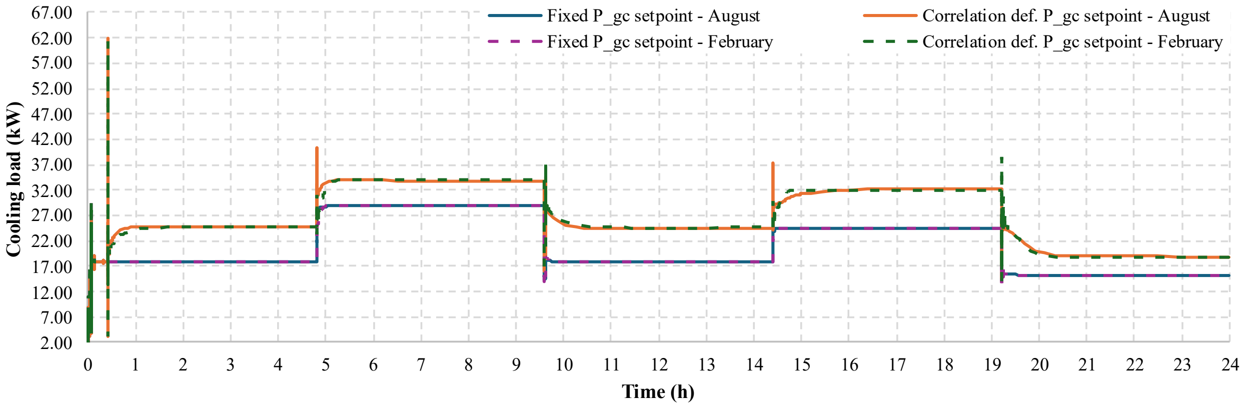


***Figure 7.*** *Cooling load dynamic response (superheating degree = 10 K).*

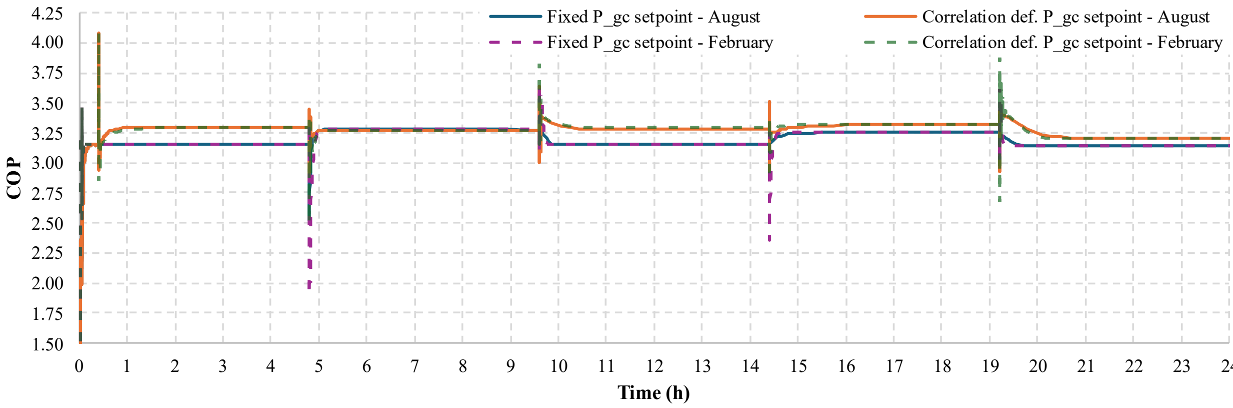


***Figure 8.*** *COP dynamic response (superheating degree = 10 K).*

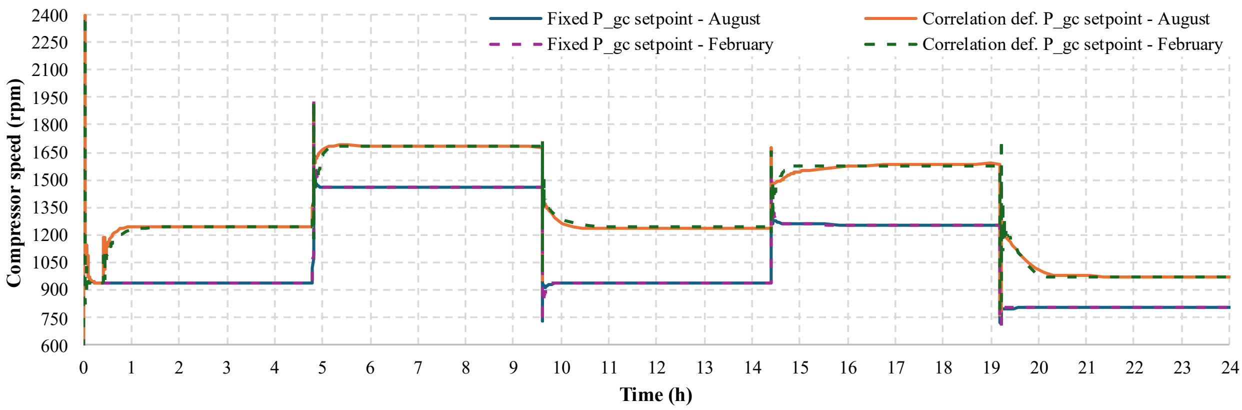


***Figure 9.*** *Compressor speed dynamic response (superheating degree = 10 K).*

In addition, it was found that the developed correlation increases the daily averaged COP by about 2.3 % on both considered days compared to the non-optimal conditions.

## 3.4 System operational cost analysis

To analyse the system operational cost, the total cooling and heating energy demand was calculated over a 24 h operational cycle on the two previously mentioned days. Then, considering the actual variable price of electricity in Denmark (see Figure 10) the energy consumption was calculated and the results are presented in Table 4. Heating and cooling loads were both considered useful; thus, the "useful energy" reported in Table 4 is the sum of the heating and cooling loads as presented in Eq. (3).

$$Q_{useful} = Q_{des} + Q_{evap} \qquad (3)$$

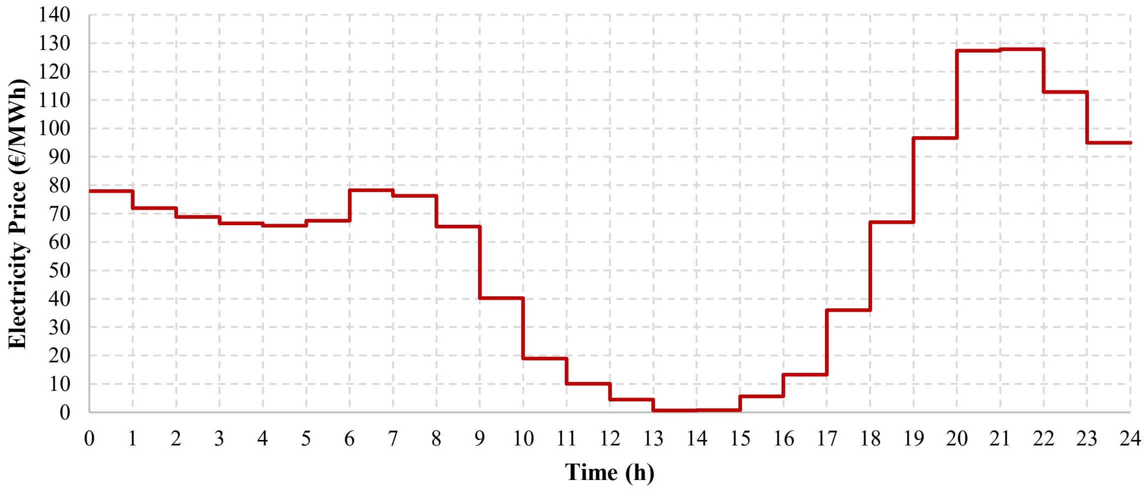


***Figure 10.*** *Actual electricity price in Denmark [9].*

Operating at the optimal pressure resulted in a 28.2 % larger evaporator load (see Figure 7), thereby reducing the useful energy cost by 3.2 % on 8 February and by 4.4 % on 4 August and maintaining the same heating capacity.

***Table 4.*** *Operational cost comparison (superheating degree = 10 K).*

| Day | Mode | Daily heating energy (MWh) | Daily cooling energy (MWh) | Daily useful energy cost (€/MWh) |
|---|---|---|---|---|
| 4 August | Fixed Pressure | 0.09 | 0.50 | 17.65 |
| | Optimal Pressure | 0.09 | 0.64 | 16.87 |
| 8 February | Fixed Pressure | 0.09 | 0.50 | 17.48 |
| | Optimal Pressure | 0.09 | 0.64 | 16.92 |

# 4. Conclusions

Ejector-based transcritical R744 heat pumps represent a sustainable amd high-performance alternative to conventional fossil-fuel boilers in dairy applications, while also meeting on-site cooling requirements. Their effective operation, however, depends on an advanced control approach capable of accurately regulating the system high-side pressure to ensure optimal efficiency across varying operating conditions. In this study, a real-time control strategy has been developed and tested using a milk processing facility as the case study. The analysed scenario has included a cooling requirement at 4 °C for milk chilling and a heating requirement at 72 °C for milk pasteurisation.

The findings highlight the critical role of high pressure in achieving optimal heat pump performance. The results show that a static gas cooler pressure setpoint is inadequate, as operating conditions vary even under constant load. By systematically mapping relevant parameters, a correlation has been developed to enable dynamic adjustment of the high pressure setpoint in ejector-based heat pumps based on the evaporator pressure and the R744 gas cooler/condenser outlet temperature. Furthermore, the correlation has shown to improve the daily average COP by approximately 2.3 % on both analyzed days (8 February and 4 August) compared to non-optimal operating conditions in Hobro (Denmark). Lastly, applying the optimal high pressure correlation reduces the cost of useful energy by at least 3 % on the selected days, while increasing the cooling load by 28 % relative to the case with the same heating demand.


# Acknowledgments

The research leading to these results has received funding from Fonden for Retfærdig Omstilling under the grant agreement No. FRO-23-0026 (Project: ULTRA).


# Nomenclature

| | |
|---|---|
| CIP | cleaning in process |
| COP | coefficient of performance (-) |
| DOE | design of experiment |
| GHG | greenhouse gas |
| GWP | global warming potential |
| $P$ | pressure, bar |
| $\dot{Q}$ | heat transfer rate, kW |
| $Q$ | heat transfer, MWh |
| $T$ | temperature, °C |
| $\dot{W}$ | power, kW |

#### Subscripts and superscripts

| | |
|---|---|
| $comp$ | compressor |
| $des$ | de-superheater |
| $evap$ | evaporation |
| $GC$ | gas cooler/condenser |

# References


[1] Singh, S., Dasgupta, M.S., 2017. $CO_2$ heat pump for waste heat recovery and utilization in dairy industry with ammonia based refrigeration. Int. J. Refrig. 78, 108-120.

[2] Gullo, P., Kærn, M.R., Haida, M., Smolka, J., Elbel, S., 2020. A review on current status of capacity control techniques for two-phase ejectors. Int. J. Refrig. 119, 64-79.

[3] Liu, F., Deng, J., Pan, W., 2018. Model-based Dynamic Optimal Control of an Ejector Expansion $CO_2$ Heat Pump Coupled with Thermal Storages. Energy Procedia 152, 156-161.

[4] Dasi, K., Singh, S., A.M., G., Maiya, M.P., Hafner, A., Banasiak, K., Neksa, P., 2020. Performance evaluation of ejector based $CO_2$ system for simultaneous heating and cooling application in an Indian dairy industry. Therm. Sci. Eng. Prog. 20, 100626.

[5] F-Chart Software, 2025. Engineering Equation Solver (EES), Academic Professional version 10.833. Available at: <http://www.fchart.com/ees/> [accessed 14.1.25].

[6] MathWorks, 2024. Inc. MATLAB version: 24.2 (R2024b). Available at: <https://www.mathworks.com> [accessed 14.1.25].

[7] Bell, I.H., Wronski, J., Quoilin, S., Lemort, V., 2014. Pure and Pseudo-pure Fluid Thermophysical Property Evaluation and the Open-Source Thermophysical Property Library CoolProp. Ind. Eng. Chem. Res. 53(6), 2498-2508.

[8] Kornhauser, A.A., 1990. The Use of an Ejector as a Refrigerant Expander. Proceedings of the International Refrigeration and Air Conditioning Conference, Purdue, USA, Paper 82.

[9] Ember, 2026. *European Wholesale electricity Price Data | Ember*. Available at: <https://ember-energy.org/data/european-wholesale-electricity-price-data/> [accessed 16.1.25].